Uniaxial fatigue study of a natural-based bio-composite material reinforced with fique natural fibers

Maria C. Chaves, Dayal Castro, Alberto David Pertuz Comas
Universidad Industrial de Santander. Escuela de ingeniería mecánica, Carrera 27, Calle 9. Bucaramanga, Colombia
camilachaves2311@gmail.com, https://orcid.org/0009-0003-8959-0878
dayalcastro@gmail.com, https://orcid.org/0000-0002-5127-4904
apertuzc@uis.edu.co, https://orcid.org/0000-0002-9130-6528

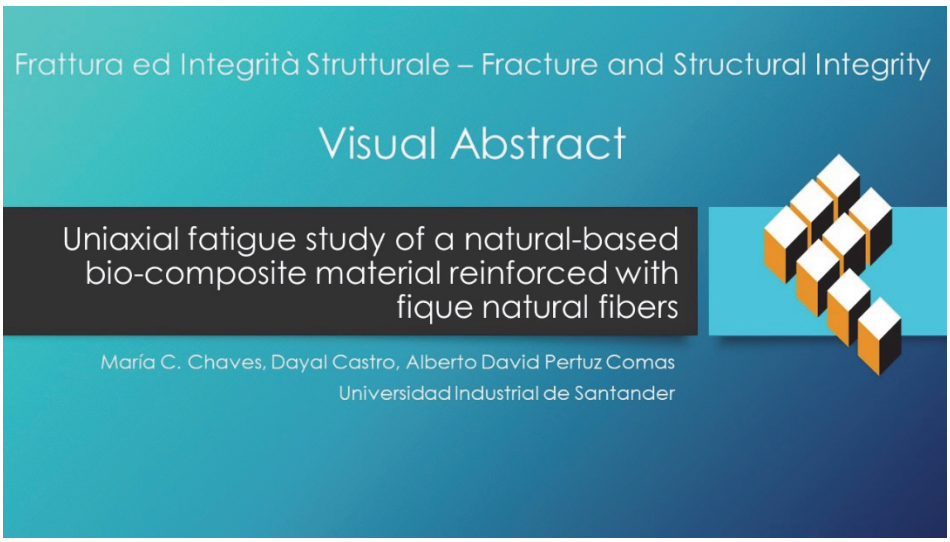

Citation: Chaves, M. C., Castro, D., Pertuz, A., Uniaxial fatigue study of a natural-based bio-composite material reinforced with fique natural fibers, Frattura ed Integrità Strutturale, 68 (2024) 94-108.

Received: 19.11.2023
Accepted: 13.01.2024
Published: 20.01.2024
Issue: 04.2024

KEYWORDS. Uniaxial fatigue, Bio-composite, Natural fibers, Fique, Fiber reinforced material.

INTRODUCTION

Microplastics, a consequence of plastic degradation in the environment, have stirred global concern due to their pervasive presence in aquatic ecosystems and the atmosphere, potentially leading to adverse effects [12]. Among these microplastics, textiles and synthetic fibers constitute the most prevalent airborne particles, posing a potential threat to human health [2]. Additionally, the urgent need to curtail energy consumption and reduce reliance on fossil fuel-based materials has fueled the quest for sustainable alternatives. This endeavor has propelled the popularity of innovative materials such as bio-based polymers [36,38], natural fibers, and their derivatives. For instance, a study by Taimour et al. [42] with very particular applications researched the use of functionally graded materials (FGM) to improve the bearing performance of pinned joints in cross-ply glass fiber-reinforced epoxy laminated composites. The study found that the FGM pinned joint had higher bearing strength than the conventional pinned joints technique.

The petrochemical industry, pivotal in synthetic fiber production, stands as a significant contributor to major greenhouse gases responsible for global warming [41]. Synthetic fibers are extensively employed as reinforcements for polymer materials (FRPs), imparting superior mechanical properties. Notably nylon, polyester, fiberglass, and carbon fiber rank among the most favored commercial fibers due to their desirable mechanical properties. However, their use poses a significant pollution source, as FRPs reinforced with synthetic fibers exhibit poor biodegradability and their manufacturing processes contribute to pollution in various ways [9]. El-Sagheer et al. [20] studied the flexural and fracture behaviors of beam-like specimens made of conventional and functionally graded (FG) PCMs. Their research explores the flexural and fracture behaviors of beam-like specimens manufactured from both conventional and functionally graded (FG) PCMs. Three distinct patterns of FG-PCMs —linear, non-linear, and stepwise/layered— resulting from fiber distribution throughout the depth were developed using long glass fiber-reinforced epoxy. Employing a three-dimensional finite element method, the study illustrates the progressive damage process in both smooth and matrix-cracked specimens. Also, Atta et al. [8] researched the flexural response of functionally graded polymeric composite material (FGM) using a hand lay-up manufacturing technique. The unidirectional glass fiber-reinforced epoxy composite consisted of ten layers and had a fiber volume fraction (V_f%) ranging from 10% to 50%. The experimental results showed that the failure mechanism of FGM beams during the three-point bending loading (3PB) test initiates from tensioned layers, extending to upper layers and leading to delamination and subsequent shear failures. Ultimately, the failure occurs due to crushing in the compression zone. Delamination between layers significantly influences the rapidity of final failure in FGM beams. Numerical results underscore the importance of the gradient pattern in FGM beams for enhancing their flexural behavior. Additionally, the V_f% in the outer layers, specifically V_f% = 30, 40, or 50%, contributes to improving their flexural strength.

In response to this challenge, the advancement of natural fiber-reinforced polymeric composites (NFRPCs), also known as natural fiber composites, has gained momentum. Offering a potential substitute for synthetic fibers, they contribute to fostering a sustainable economy [14]. Natural fibers such as flax, jute, hemp, bamboo, and kenaf serve as reinforcements owing to their numerous advantages: wide availability, cost-effectiveness, high specific strength, and stiffness, while also supporting rural livelihoods [6]. Other studies include the effect of short fibers focused on the mechanical behavior of palm fiber-reinforced epoxy-based composites with different weight percentage (Wt.%) ratios, ranging from 6% to 31.6%. They also examined glass and hybrid fiber-reinforced epoxy-based composites. The research used the diametral tensile test (DTT) and the small punch test (SPT) to determine the mechanical properties of the composites. The results indicated that the natural fiber had better adhesion bonding with the epoxy than glass fiber, and the addition of palm fibers improved the mechanical properties of the epoxy compared to synthetic glass fibers [4].

Furcraea sp., colloquially known as fique and indigenous to Colombia, has been cultivated since ancient times. Traditionally its fibers were employed in sacks and tying material production, primarily by smallholder farmers [18]. Despite serving as a primary income source for many, fique faces challenges such as low selling prices and inefficient production methods due to decreased demand in recent decades. Hence, the utilization of natural fibers in material production opens new market opportunities for rural areas, stimulating their economic development [16].

However, despite the potential of natural fibers like fique, a substantial lack of information exists concerning their behavior and properties, particularly considering variations arising from their natural origin [22,24,37]. This knowledge gap impedes the complete utilization of natural fibers as composite reinforcements and inhibits their widespread adoption across diverse sectors [11,15,29].

Researchers, such as El-Sagheer et al. [19], have conducted studies to characterize natural fibers under dynamic stress conditions; the study by El-Sagheer et al. specifically aimed to predict the exact value of the fracture toughness (KQ) of fiber-reinforced polymer (FRP) by suggesting unprecedented, cracked specimens, i.e., matrix cracked (MC) specimens, to overcome the deficiency of the American Society for Testing Materials (ASTM) E1922 specimen. The MC specimens exist in the matrix (epoxy) without cutting the glass fibers behind the crack tip in the unidirectional laminated composite. While the mechanical properties of tribology have been studied, the paper aims to experimentally assess the mechanical and tribological behavior of conventional and functionally graded (FG) polymeric matrix composites reinforced with continuous glass fibers. The study used the hand lay-up technique to manufacture the composites, the small punch test (SPT), and a pin-on-disc device to examine the mechanical and wear behaviors. The results indicated that the wear rate of the FG composite was influenced by various factors, including disk speed, applied load, the number of composite layers, and average glass fiber volume fraction [3].

Therefore, characterizing the fatigue behavior of fique-reinforced composites is crucial to understanding their performance, thus positioning them as viable materials in design applications; thus, this research proposes the development of a Bio-Poxy 36 polymer matrix composite with a high carbon content reinforced with fique fabric, a plant cultivated in Colombia, using the vacuum-assisted lamination method.

MATERIALS AND METHODS

Raw materials and fiber processing

The raw materials employed in the present study were fique natural fibers and the BioPoxy 36 two-component epoxy system (resin and hardener) from EcoPoxy. The fique fibers (obtained from the leaves of the Furcraea plant native to South America) were acquired in a woven configuration from Cohilados del Fonce (marketed as coffee bags No. 10), as shown in Fig. 1a. The fique textile underwent a chemical surface treatment to improve the adhesion between the fiber and the matrix. Alkalinization with NaOH was chosen due to its low cost and effectiveness, with a concentration of 2% by weight as recommended by the literature [1,5,7,21,44] to avoid compromising the fiber's properties with a highly aggressive solution. The fibers were fully immersed in the NaOH solution (as seen in Fig. 1b) and manually stirred at 5 to 10-minute intervals to guarantee uniform treatment of the textile. Following a 30-minute exposure to the solution, the fibers were meticulously rinsed with distilled water and subsequently air-dried in the shade for 48 hours.

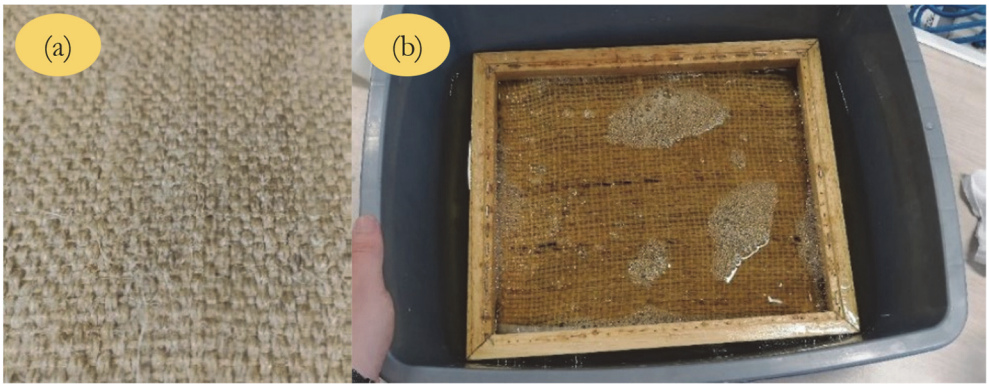

Figure 1: (a) Woven configuration of the fique fibers (b) Alkalinization process of the fique fabric.

The properties of the BioPoxy 36, as listed in the manufacturer's datasheet, are presented in Tab. 1.

Properties	Values*
Density	1.11 g/cm^3
Tensile strength	57.9 MPa
Young's Modulus	2.83 GPa
Elongation at break	2.80 %
Glass transition temperature	54 °C

Table 1: Properties of the BioPoxy 36 *According to the manufacturer's datasheet.

Tab. 2 displays the properties that were obtained during the tensile testing of samples of BioPoxy 36 resin. The observed fluctuations in the ultimate stress and Young's modulus values, when compared to the values reported by the manufacturer, suggest that storage conditions and the duration since the resin was opened may have an impact on the epoxy's properties.

Properties	Value	Coefficient of variation (%)
Ultimate strength (MPa)	23.6 ± 2.85	12.06
Strain (%)	1.19 ± 0.14	12.35
Young's modulus (GPa)	2.22 ± 0.11	4.89

Table 2: Mechanical properties of the BioPoxy 36 tested samples.

A comparison was made between the mechanical properties of the tested fique textile and other studies reported in the literature, as presented in Tab. 3. The fique fibers were considered to have a density of 0.87 g/cm³, based on a previously reported study [35]. Using this density, an estimated volumetric fiber fraction V_f of 27% was calculated for each laminate of the composite. Additionally, the estimation of the fique fiber area within the fabric was accomplished through image processing in MATLAB, facilitating the determination of fiber diameter.

Properties	Values	Reference Values*
Ultimate strength (MPa)	400.81 ± 89.68	47 - 571
Strain (%)	4.64 ± 1.62	9.8
Young's modulus (GPa)	9.4 ± 1.26	8.2 - 9.1

Table 3: Mechanical properties of the fique textile. *Values adapted from Gómez Suarez & Córdoba Tuta [23].

Composite manufacture

A modified vacuum-assisted lamination process was used to create the test BioPoxy-fique samples. The base for lamination was an 8 mm thick glass measuring 60 x 40 cm. To make demolding easier, a layer of polyvinyl alcohol was applied to the glass 24 hours before the procedure.

Initially, the resin and catalyst mixture was prepared with a volumetric ratio of 4:1 (resin: catalyst). The first layer for lamination was poured, and a plastic spreader was used to distribute it evenly. Next, a layer of fique fabric was placed over the resin. The remaining resin was poured over the fabric and spread uniformly. The complete process is shown in Fig. 2.

Figure 2: Pouring of resin layers.

After all the layers were in place, an acrylic sheet was put over the fabric (as shown in Fig. 3a). Then, a breather layer was added to cover the entire work area. After that, a pneumatic hose was placed in position using butyl tape (as shown in Fig. 3b). Finally, the vacuum sealing plastic was put over the acrylic, with small tabs left to avoid tension in the plastic (as shown in Fig. 3c). The final configuration is illustrated in Fig. 3d.

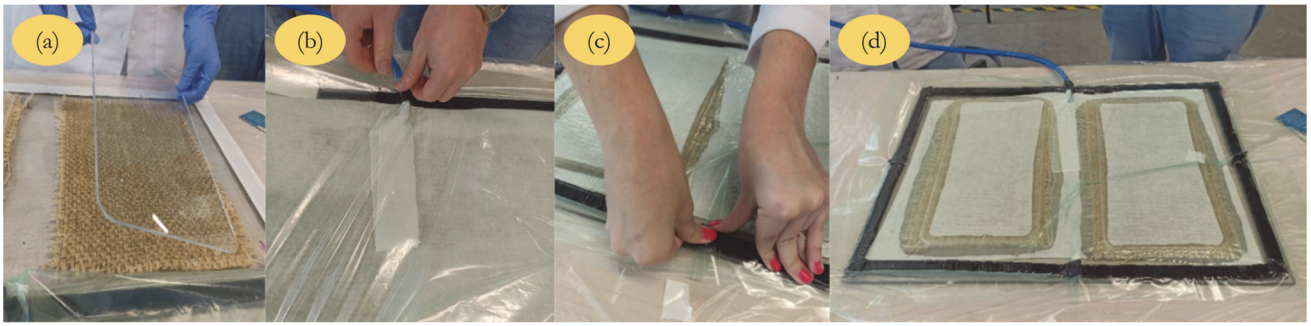

Figure 3: Bag sealing and final setup of the process.

Tensile tests

The tensile tests were conducted following the ASTM D3039 standard for polymer matrix composites. Rectangular-shaped specimens were laser-cut to dimensions of 13 x 2.5 cm. To ensure accuracy, an extensometer with a gauge length of 25 mm was used, along with an MTS machine operating at a speed of 2 mm/min.

Fatigue tests

The fatigue tests were carried out using a universal testing machine on samples with the geometry shown in Fig. 4, following the guidelines established in the ASTM 3479 standard, at a frequency of 5 Hz. To calculate the material strain, the displacement data recorded by the machine's load heads was used.

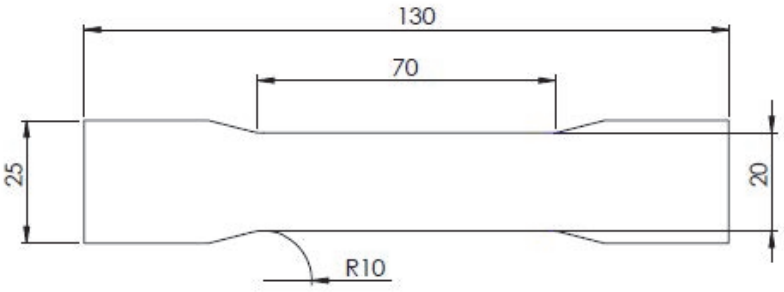

Figure 4: Geometry and dimensions (mm) of fatigue specimens.

To address the issue of conflicting stiffness behavior commonly found in fiber-reinforced natural composites, prior studies [13,30,32] have emphasized the importance of cyclic loading with a constant strain amplitude. This approach is better suited for analyzing the fatigue strength of composites as it avoids the introduction of new variables that could affect fatigue life estimation, such as variable strain rates seen in constant amplitude stress tests [33,34,39]. Given the viscoelastic nature of BioPoxy 36 and the high standard deviation of displacements, tension tests at displacement percentages of 130%, 115%, 95%, and 85% of the maximum measured strain were conducted. This enabled us to analyze both over and under the static strain limit, employing a strain ratio (R) of 0.1 throughout the experiments.

Stiffness degradation

The purpose of this analysis was to investigate how the material's stiffness changes over time. For this purpose, stiffness values were compared at various stages of the fatigue test, enabling the assessment of stiffness degradation. Stress-strain hysteresis curves generated during the fatigue tests were analyzed to determine the dynamic Young's modulus, also known as the secant modulus. Subsequently, a comparison between the initial stiffness (E_0) and the residual stiffness (E) was conducted at specific intervals of fatigue life to quantify the extent of stiffness loss. The residual stiffness was calculated considering the maximum and minimum stress and strain values obtained from the complete load-unload cycle associated with each analyzed cycle, as illustrated in Fig. 5.

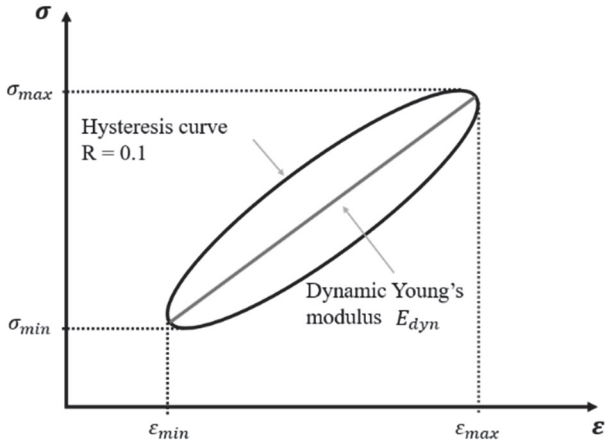

Figure 5: Calculation of the dynamic Young's modulus from the stress-strain curve.

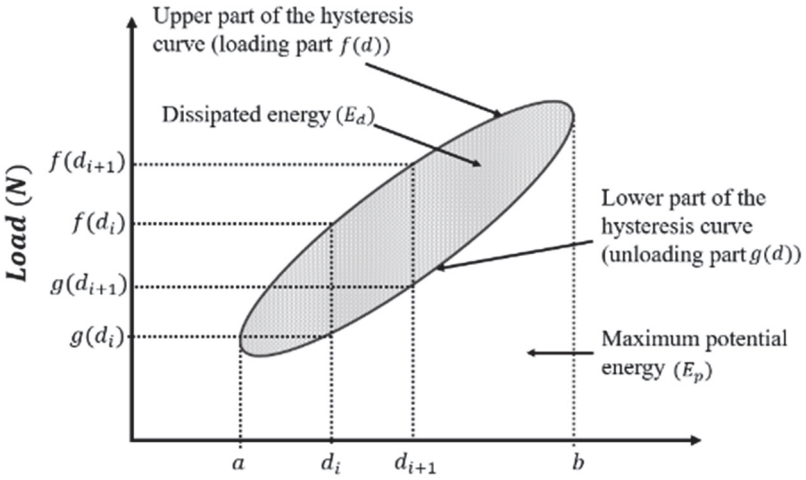

Figure 6: Load-displacement hysteresis loop and mechanical parameters measured during the fatigue cycles.

Loss factor and energy dissipation

The area enclosed within each hysteresis curve, as observed in Fig. 6, represents the amount of energy (E_d) that has been dissipated during that cycle. This area is a useful indicator of the material's condition. The dissipated energy is calculated as the difference between the total energy input required to induce deformation (E_p) and the energy recovered. To evaluate damage progression in composite materials, the damping or loss factor (η) is widely used as it is more sensitive in detecting changes compared to stiffness evolution. The damping factor quantifies the proportion of dissipated energy with the potential energy of a given fatigue cycle [25,26]. It can be calculated using the following equation:

$$\eta = \frac{E_d}{2\pi E_p} \tag{1}$$

Low-cycle fatigue model

The modified Coffin-Manson model for low-cycle fatigue was employed in this study to predict the material's service life under cyclic loading conditions. This model takes into account both elastic and plastic strain and is based on the correlation between strain amplitude and the number of cycles to failure. The model is represented by the following equation:

$$\frac{\Delta\varepsilon}{2} = \frac{\Delta\varepsilon_e}{2} + \frac{\Delta\varepsilon_p}{2} = \sigma'_f \left(2N_f\right)^b + \varepsilon'_f \left(2N_f\right)^c \tag{2}$$

When implementing this model, two key parameters were identified: the fatigue strength coefficient (σ'_f), given by the true stress at failure, and the fatigue ductility coefficient (ε'_f). These parameters represent the specific properties of the material being studied.

RESULTS AND ANALYSIS

The results presented herein offer a comprehensive analysis of the mechanical behavior, fatigue resistance, stiffness loss, loss factor, energy dissipation, strain-life relationship, and fracture morphology of the BioPoxy-fique composite material in comparison to BioPoxy 36 resin. Below is an analysis summarizing the key findings:

Tensile properties

The BioPoxy 36 matrix demonstrates a linear elastic behavior until failure, which occurs suddenly due to its inherent brittleness, as illustrated in the stress-strain curves of Fig. 7.

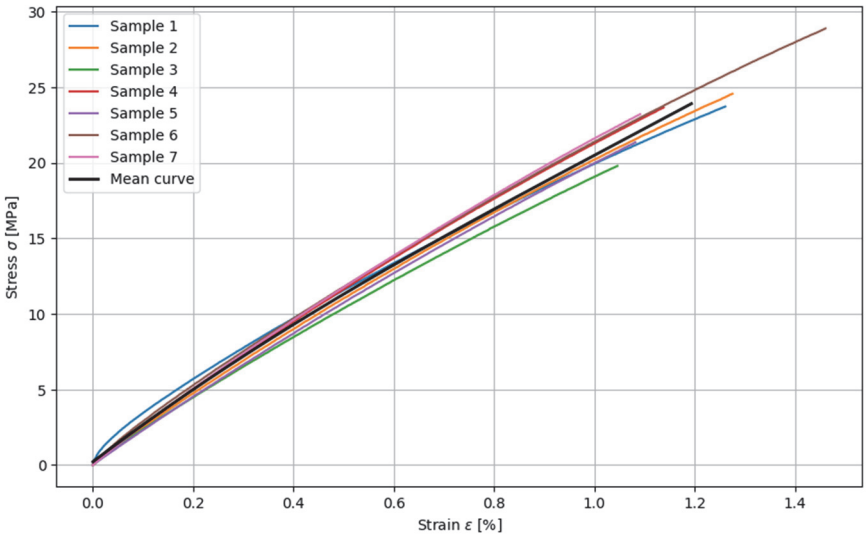

Figure 7: Stress-strain curves of the BioPoxy 36 resin.

The behavior of the BioPoxy 36 resin demonstrated linear elastic characteristics until failure, specifically up to a 0.3% strain. This behavior can be attributed to its inherent brittleness, representing the elastic and reversible response of the bio-composite. In contrast, the BioPoxy-fique composite, shown in Fig. 8) exhibited a two-stage non-linear trend: an initial linear phase (elastic) succeeded by a non-linear phase (plastic) until failure. This plastic behavior indicated the formation and progression of damage mechanisms within the fibers, matrix, or their interface. Similar behavior in resin and fiber composites has been extensively discussed by various authors [10,23,26]. The mechanical properties of the BioPoxy-fique composite are listed in Tab. 4.

Properties	Value	Coefficient of variation (%)
Ultimate strength (MPa)	34.28 ± 3.21	9.36
Strain (%)	2.87 ± 0.64	22.38
Young's modulus (GPa)	2.82 ± 0.23	8.31

Table 4: Mechanical properties of the BioPoxy-fique composite.

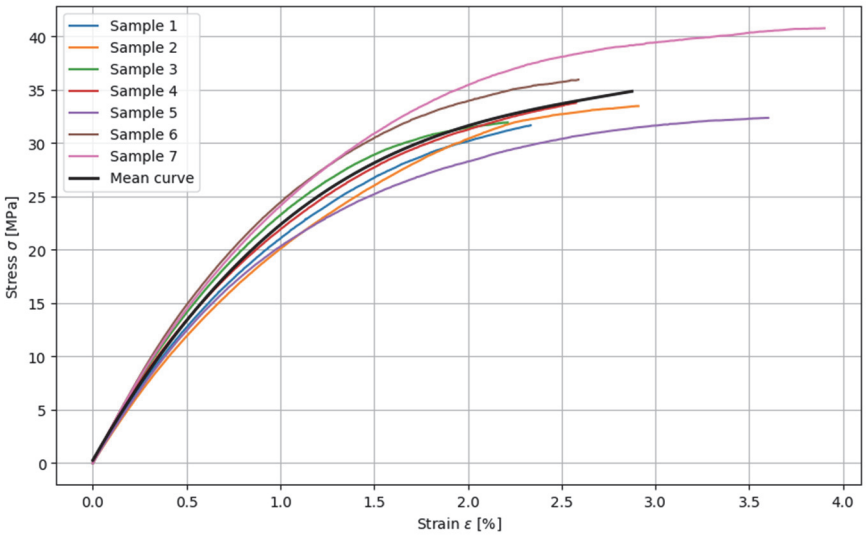

Figure 8: Stress-strain curves of the BioPoxy-fique composite by the vacuum bagging method.

Fig. 9 illustrates the comparison between the composite and BioPoxy 36 resin. The static mechanical properties of the composite exhibit a significant increase in ultimate strength, estimated at a 45% increase in ultimate stress, a remarkable 145% increase in strain, and a 27% increase in Young's modulus compared to the BioPoxy 36 resin.

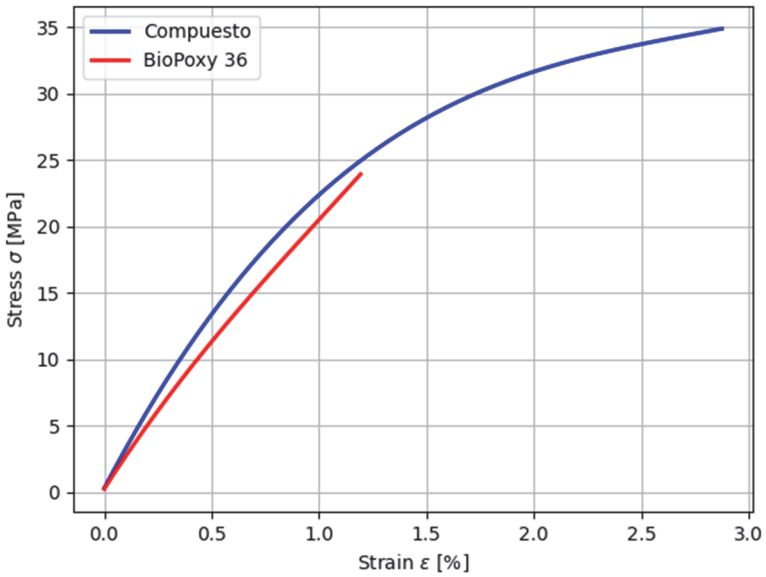

Figure 9: Comparison between stress-strain curves of the composite and BioPoxy 36 resin.

Other studies, such as those by [24], delved into the influence of natural fiber twisting on mechanical properties, while [32] provided computational models for these properties. Although these studies primarily focused on flax fibers, their findings remain comparable to the results obtained in this work, even though flax is a more extensively studied fiber than fique.

Fatigue behavior

During the fatigue tension-tension tests, the stress-strain behavior was examined by recording 40 real-time data points for each load-unload cycle. Fig. 10 presents the hysteresis curves for cycles 1, 10, 10^2, 10^3, 10^4, and 10^5, at an 85% level of the maximum strain observed in the static tests.

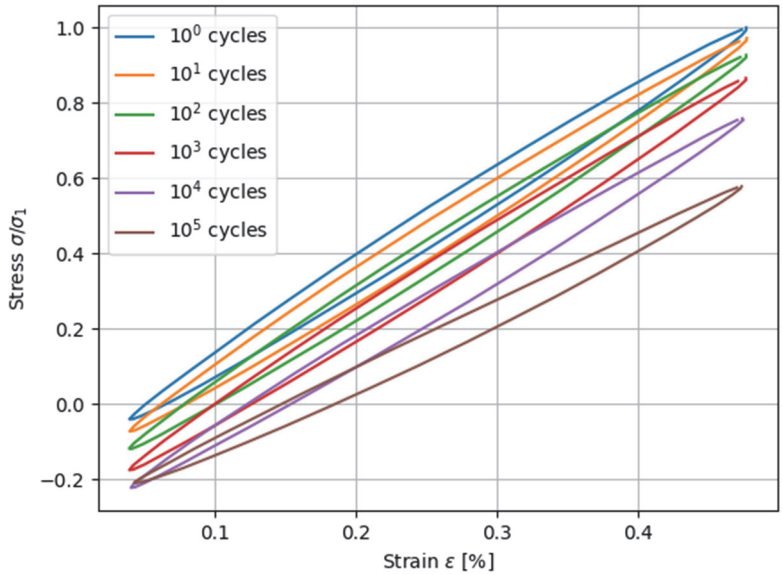

Figure 10: Stress-strain hysteresis curves for 85% of the maximum strain. (Where σ_1 denotes the maximum stress recorded in the first cycle).

It is worth noting that during the initial cycles, the hysteresis curves exhibited larger areas and maximum loads compared to subsequent cycles. This suggests an increase in damage activity, particularly at the fiber-matrix interface, and the propagation of damage within the composite. It is important to acknowledge that limited research has been conducted on the fatigue behavior of natural fiber fique composites. However, studies by authors such as Dobah et al. [17], focusing on jute composite reinforcement, and the extensive exploration of flax by Haggui et al. [26] and Goumghar et al. [25] served as references guiding our study. Comparing the results obtained in our study with theirs showcases the promising performance of fique as a reinforcement material for composites.

Stiffness loss

In Fig. 11, the stiffness evolution is illustrated in relation to the number of cycles for every strain amplitude tested. To facilitate understanding, the dynamic modulus was normalized by dividing it by the initial value (E_0), which represents the modulus in the first load-unload cycle of the stress-strain curves. Across all scenarios, a two-stage decrease in stiffness is noticeable, displaying a proportional trend to the applied strain amplitude.

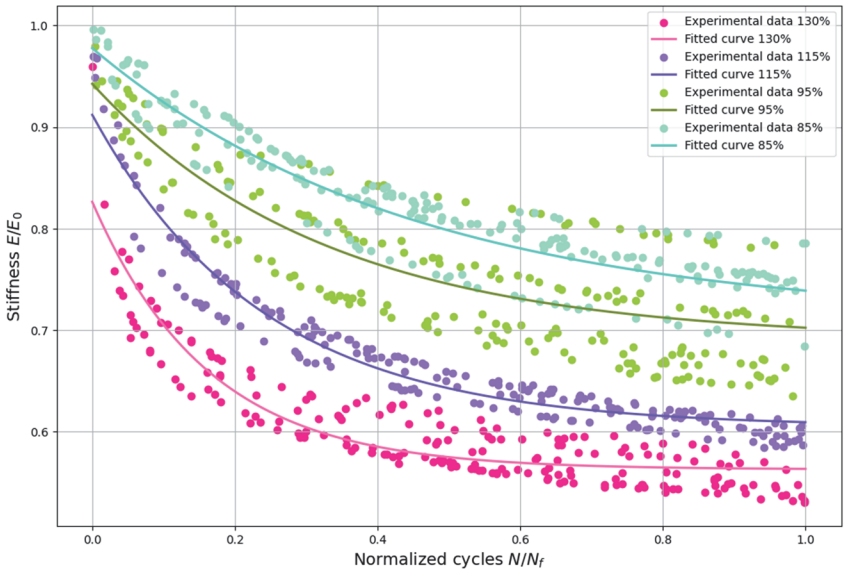

Figure 11: Evolution of the dynamic modulus for all strain amplitudes.

During the initial stage of material life at all levels of strain amplitude, a systematic softening is observed, which stabilizes in the following stage [33,39]. This finding suggests that the damage mechanisms are more prominent in the early stages of fatigue, before reaching the threshold of 0.4 N/N_f. At higher levels of strain amplitudes, a significant loss of stiffness exceeding 40% is evident.

The observed stiffness degradation in the initial cycles contradicts the findings of previous studies [30,31,39] conducted under constant stress amplitude conditions. This discrepancy is attributed to the progressive increase in strain amplitude over the fatigue life of the material. It has been reported that this significant increase in strain can counterbalance the degradation caused by internal damage mechanisms during the loading cycles, leading to a misleading perception of structural improvement in the material [33]. However, it is worth noting that this phenomenon is not evident in similar tests conducted at high frequencies [28].

Tab. 5 provides a comparison between the initial dynamic moduli for all strain amplitudes and the static Young's modulus obtained from the tests. A noticeable disparity is observed between the static modulus and the values obtained from fatigue testing. It is worth highlighting that the loading rate employed in the static tests, which was 2 mm/min, is significantly lower compared to the rate used in the fatigue tests, conducted at a frequency of 5 Hz. This discrepancy in loading rates accounts for the observed increment in stiffness.

Loss factor and energy dissipation

The monitoring of energy dissipation serves as a reliable indicator for assessing the crack propagation velocity in the composite. The area enclosed within the hysteresis curve provides a direct measure of the energy dissipated during each

cycle, which correlates with the applied strain level. Similarly, the area under the loading curve represents the maximum potential energy. Fig. 12 illustrates the progressive changes in the loss factor for each tested strain level, thereby establishing a clear relationship between these two forms of energy.

Testing parameters	Elastic modulus (GPa)	Coefficient of variation (%)
Tensile test	2.82 ± 0.23	8.31
Fatigue 130%	3.92 ± 0.13	3.34
Fatigue 115%	4.35 ± 0.13	2.91
Fatigue 95%	4.29 ± 0.34	7.88
Fatigue 85%	4.27 ± 0.07	1.77

Table 5: Comparison of static and dynamic test modulus.

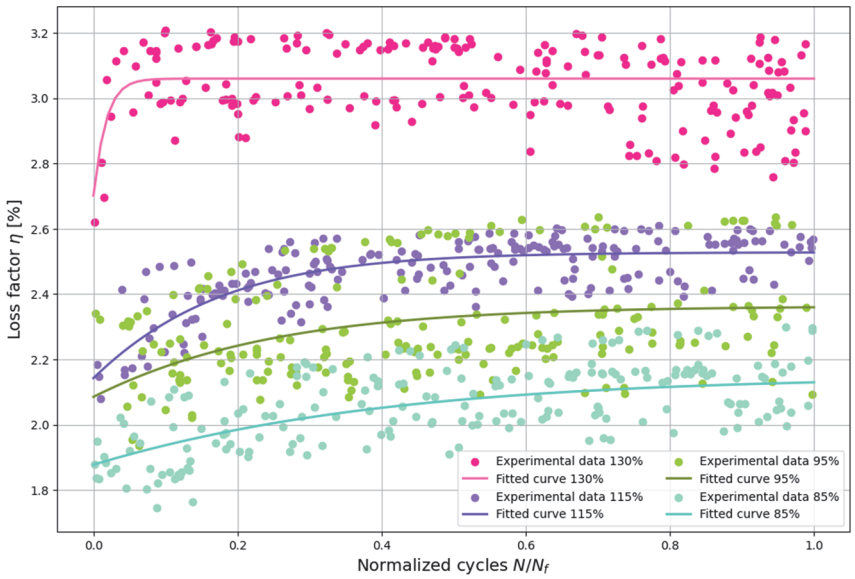

Figure 12: Evolution of the loss factor as a function of the number of normalized cycles.

Similar to the observed behavior in stiffness loss, it is possible to identify two stages. In the first stage, there is a rapid decrease in energy, followed by a second stage of stabilization where degradation is minimal. The loss factor is commonly regarded as a more precise indicator of the degradation process in composite materials due to its higher sensitivity compared to stiffness evolution [25].

The energy dissipated per cycle is generated through internal friction, which produces heat, and micro-plastic strain, which involves crack formation [25–27]. Internal friction increases proportionally with the applied strain level, implying that energy dissipation is higher at higher strain levels.

Strain-life curve

In the analysis of the strain-life relationship, the stabilization of the loss factor was used as the failure criterion. It was observed that stabilization occurs at different values of normalized cycles depending on the strain percentage: 0.8 N/N_f for 85% strain, 0.6 N/N_f for 95% strain, 0.4 N/N_f for 115%, and 0.2 N/N_f for 130% strain. Notably, as the strain percentage increases, the stabilization of the loss factor is achieved more rapidly. The strain-life curve, depicted in Fig. 13, was fitted using the Coffin-Manson model, described previously.

SEM analysis

The analysis of fracture surfaces was conducted through scanning electron microscopy (SEM). Fig. 14 illustrates the cross-sectional surface of a specimen that did not undergo complete fracture during fatigue tests. Regions rich in resin are evident,

accompanied by surface defects like bubbles, a byproduct of the manufacturing process. Additionally, the matrix shows areas of fiber-matrix adhesion and fiber-matrix debonding, an occurrence assumed to be a consequence of stress transfer between them.

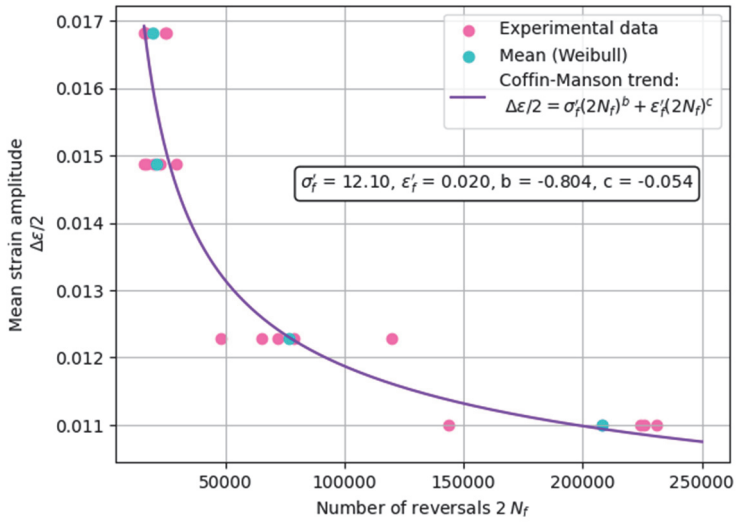

Figure 13: Strain-life curve for the BioPoxy-fique composite.

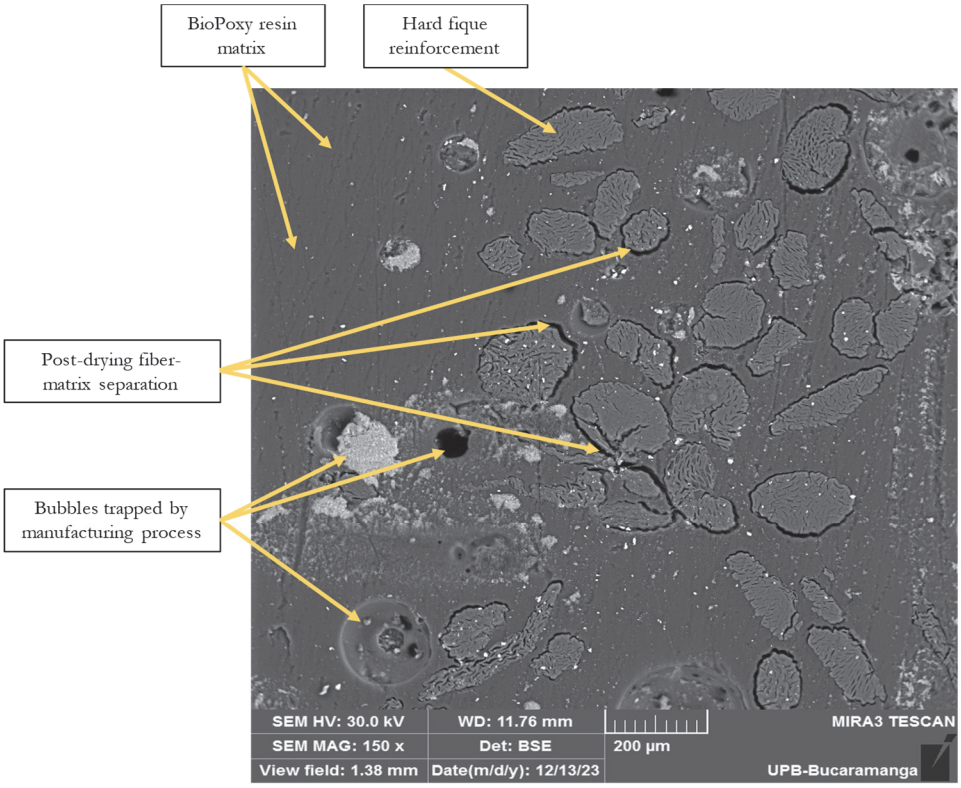

Figure 14: Cross-section of a sample tested at a 130% strain level.

Since complete fracture was not achieved during fatigue tests, some samples were ruptured using liquid nitrogen. Fig. 15 reveals fiber pullout, a phenomenon dependent upon the strength of the fiber-matrix union and the associated stress transfer mechanisms. The fiber ends exhibit characteristics of a brittle failure mode. Additionally, the presence of river marks is noteworthy, indicating damage to the matrix. These marks signify a loss of cohesion in the material, serving as evidence of structural degradation.

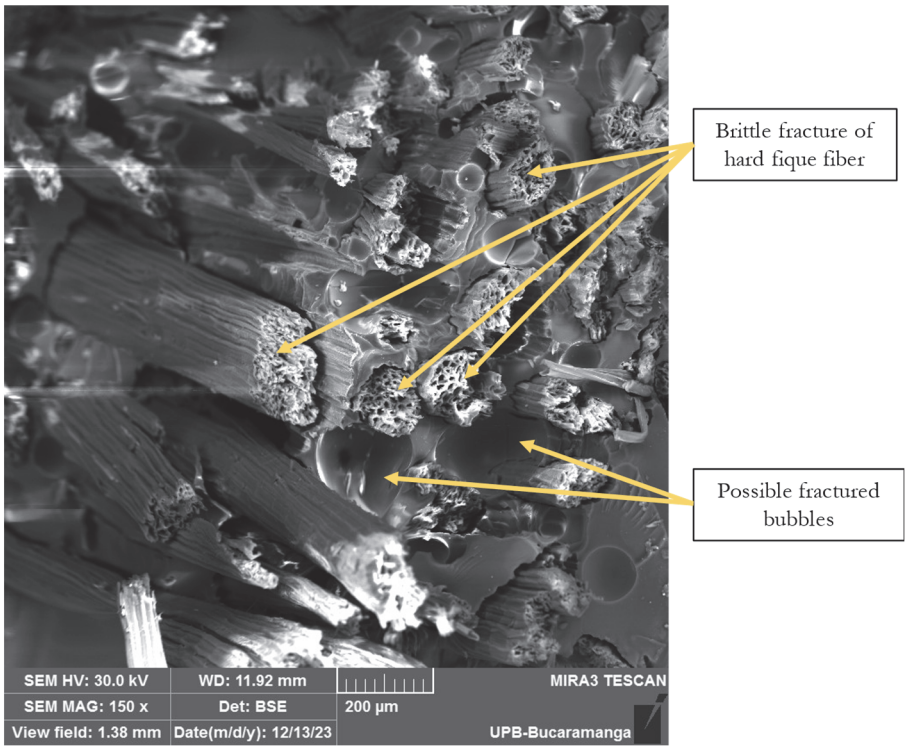

Figure 15: Rupture of longitudinal fibers.

Furthermore, Fig. 16a illustrates the rupture of a bundle of transverse fibers, displaying a failure process characterized by the rupture of individual fibers known as singlets. A critical cluster of fiber breakage is formed as seen in Fig. 16b, eventually leading to material failure [43]. Again, surface defects inherent to the manufacturing process are visible.

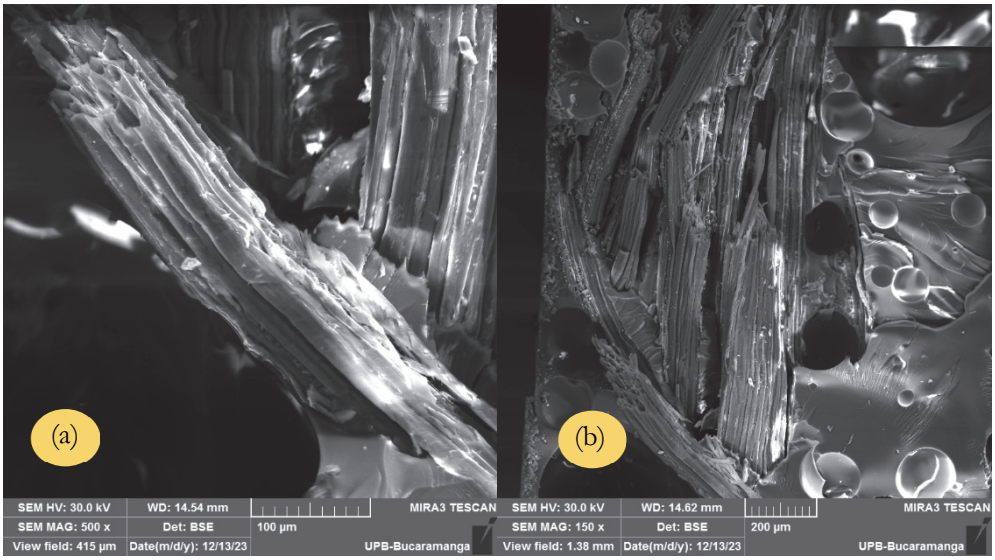

Figure 16: Rupture of transversal fibers.

Fig. 17 illustrates the entire fracture surface in the testing area, revealing wear marks attributed to fatigue. The detachment of transverse fibers from the matrix is observed, indicating a variable strength of the fiber-matrix bond across the surface. The BioPoxy-Fique composite is estimated to have a fiber volumetric fraction (V_f) of 27%. In other studies, the fiber content in the composite has been found to influence its fatigue failure mechanisms under tension-tension loading. Studies have demonstrated that composites with a low fiber content exhibit a higher generation of surface cracks in the matrix during the early stages of fatigue [40].

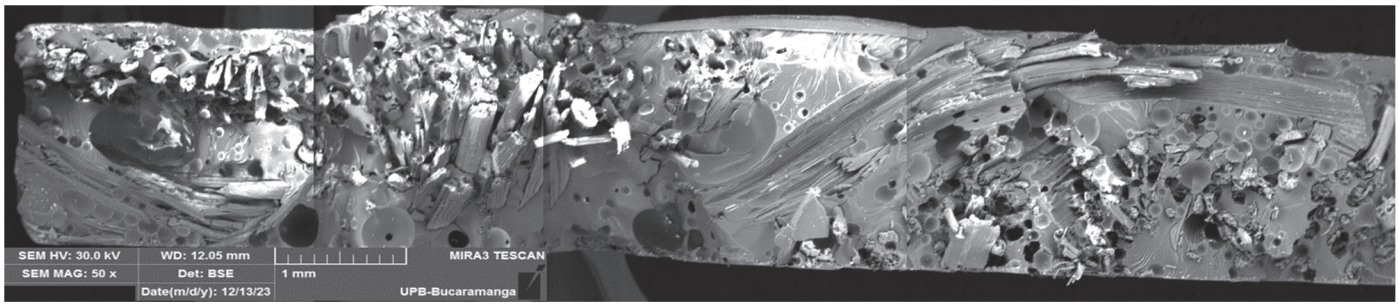

Figure 17: General view of fracture surface at a 95% strain level.

The study offers valuable insights into the mechanical behavior and fatigue performance of the BioPoxy-fique composite, which has great potential for various applications, particularly in structural materials. The thorough analysis highlights the composite's mechanical behavior, fatigue resistance, stiffness loss, energy dissipation, strain-life relationship, and fracture morphology. It also emphasizes the influence of strain amplitude, loading rates, and fiber content on the material's structural integrity and failure mechanisms.

Conclusions

The static tests revealed a nonlinear response in the stress-strain curves of the BioPoxy-fique compound, indicating two distinct stages of behavior. The first stage exhibited elastic and reversible behavior, while the second stage displayed plastic behavior associated with the development of damage mechanisms in the fibers, matrix, or interface. Two degradation stages were identified in the BioPoxy-fique compound. In the first stage, the material underwent progressive softening, while in the second stage, the degradation stabilized. The loss factor and stiffness degradation criteria were used to characterize these stages, resulting in the following parameters for the Coffin-Manson equation in the strain-life curve: $\sigma'_f = 12.10$, $\varepsilon'_f = 0.02$, $b = -0.804$ y $c = -0.054$. However, the low cycling analysis could be further enhanced by considering the viscoelastic contribution of the BioPoxy matrix, potentially modifying the frequency of testing to capture a more comprehensive understanding of its behavior.

Comparing the BioPoxy-fique composite with the BioPoxy 36 resin, significant improvements were observed in the mechanical properties of the composite. The ultimate stress increased by 45%, the maximum strain by 145%, and Young's modulus by 27% with the addition of natural fique fibers as reinforcement. Furthermore, the influence of storage conditions on the response of BioPoxy 36 necessitates further exploration, particularly regarding the effects of environmental humidity on its composition and mechanical properties. Understanding these variations is imperative for better control and optimization of the manufacturing process. Moreover, given the sensitivity of mechanical behavior to different fiber suppliers, a comprehensive study on fique suppliers in Colombia becomes essential. This investigation will provide valuable insights into the variability of mechanical properties, ensuring consistent and reliable manufacturing processes.

The findings emphasize the importance of considering specific damage stages and the influence of strain amplitude on the lifespan of the material. It is recommended to avoid using the initial dynamic modulus as a design criterion due to its significant degradation in the first stage of fatigue life. Instead, the value of the second stage, where degradation is minimal, should be considered.

References

[1] Vinod, A., Sanjay, M. R., Siengchin, S. (2021). Fatigue and thermo-mechanical properties of chemically treated Morinda citrifolia fiber-reinforced bio-epoxy composite: A sustainable green material for cleaner production, J Clean Prod, 326. DOI: 10.1016/J.JCLEPRO.2021.129411.

[2] Akanyange, S.N., Lyu, X., Zhao, X., Li, X., Zhang, Y., Crittenden, J.C., Anning, C., Chen, T., Jiang, T., Zhao, H. (2021). Does microplastic really represent a threat? A review of the atmospheric contamination sources and potential impacts, Science of the Total Environment, 777. DOI: 10.1016/J.SCITOTENV.2021.146020.

[3] Alhazmi, W., Jazaa, Y., Althahban, S., Mousa, S., Abu-Sinna, A., Abd-Elhady, A., Sallam, H.E.D., Atta, M. (2022). Mechanical and Tribological Behavior of Functionally Graded Unidirectional Glass Fiber-Reinforced Epoxy Composites, Polymers (Basel), 14(10), p. 2057. DOI: 10.3390/POLYM14102057/S1.
[4] Alomari, A.; S.;, Vantadori, S.;, Alhazmi, W.H.;, Abd-Elhady, A.A.;, Sallam, H., Mousa, S., Alomari, A.S., Vantadori, S., Alhazmi, W.H., Abd-Elhady, A.A., El-Din, H., Sallam, M. (2022). Mechanical Behavior of Epoxy Reinforced by Hybrid Short Palm/Glass Fibers, Sustainability 2022, 14, 9425, DOI: 10.3390/SU14159425.
[5] Alsuwait, R.B., Souiyah, M., Momohjimoh, I., Ganiyu, S.A., Bakare, A.O. (2023). Recent Development in the Processing, Properties, and Applications of Epoxy-Based Natural Fiber Polymer Biocomposites, Polymers (Basel), 15(1). DOI: 10.3390/POLYM15010145.
[6] Alves Fidelis, M.E., Pereira, T.V.C., Gomes, O.D.F.M., De Andrade Silva, F., Toledo Filho, R.D. (2013). The effect of fiber morphology on the tensile strength of natural fibers, Journal of Materials Research and Technology, 2(2), pp. 149–157. DOI: 10.1016/J.JMRT.2013.02.003/.
[7] Andrew, J.J., Dhakal, H.N. (2022). Sustainable biobased composites for advanced applications: recent trends and future opportunities – A critical review, Composites Part C: Open Access, 7. DOI: 10.1016/J.JCOMC.2021.100220/.
[8] Atta, M., Abu-Sinna, A., Mousa, S., Sallam, H.E.M., Abd-Elhady, A.A. (2022). Flexural behavior of functionally graded polymeric composite beams, Journal of Industrial Textiles, 51(3_suppl), pp. 4268S-4289S. DOI: 10.1177/15280837211000365/ASSET/IMAGES/LARGE/10.1177_15280837211000365-FIG11.JPEG.
[9] Bachchan, A.A., Das, P.P., Chaudhary, V. (2020). Effect of moisture absorption on the properties of natural fiber reinforced polymer composites: A review, Mater Today Proc, 49, pp. 3403–3408. DOI: 10.1016/J.MATPR.2021.02.812.
[10] Baets, J., Plastria, D., Ivens, J., Verpoest, I. (2014). Determination of the optimal flax fibre preparation for use in unidirectional flax-epoxy composites, Journal of Reinforced Plastics and Composites, 33(5), pp. 493–502. DOI: 10.1177/0731684413518620.
[11] Barros, F.A., Gamboa, J.M., Diaz-Ramirez, G.A., González-Estrada, O.A., Cruz, R.A. (2019). Numerical and experimental study of flexural behaviour in polymer composite materials reinforced with natural fique textiles, J Phys Conf Ser, 1247(1). DOI: 10.1088/1742-6596/1247/1/012001.
[12] Bellasi, A., Binda, G., Pozzi, A., Galafassi, S., Volta, P., Bettinetti, R. (2020). Microplastic contamination in freshwater environments: A review, focusing on interactions with sediments and benthic organisms, Environments - MDPI, 7(4). DOI: 10.3390/ENVIRONMENTS7040030.
[13] Bensadoun, F., Vallons, K.A.M., Lessard, L.B., Verpoest, I., Van Vuure, A.W. (2016). Fatigue behaviour assessment of flax-epoxy composites, Compos Part A Appl Sci Manuf, 82, pp. 253–266. DOI: 10.1016/J.COMPOSITESA.2015.11.003.
[14] Campilho, R.D.S.G. ed. (2015). Natural Fiber Composites, CRC Press, DOI: 10.1201/b19062.
[15] Castro, D., Pertuz, A., León-Becerra, J. (2022). Mechanical behavior analysis of a vertical axis wind turbine blade made with fique-epoxy composite using FEM, Procedia Comput Sci, 203, pp. 310–317. DOI: 10.1016/J.PROCS.2022.07.039/.
[16] Díaz, I., Fromm, I. (2019). The rebirth of natural fibers? Analysis of market potential for fique (furcraeaandina) production in Santander, Colombia, Journal of Nutritional Health & Food Engineering, 9(2), pp. 56–60. DOI: 10.15406/JNHFE.2019.09.00326.
[17] Dobah, Y., Bourchak, M., Bezazi, A., Belaadi, A., Scarpa, F. (2016). Multi-axial mechanical characterization of jute fiber/polyester composite materials, Compos B Eng, 90, pp. 450–456. DOI: 10.1016/J.COMPOSITESB.2015.10.030.
[18] Echeverri, R.D.E., Montoya, L.M.F., Velásquez, M.R.G. (2015). Fique en Colombia, Fique En Colombia, DOI: 10.22430/9789588743820.
[19] El-Sagheer, I., Abd-Elhady, A.A., El-Din, H., Sallam, M., Naga, S.A.R., Sallam, A.A., Naga, E.-D.M.;, Eg, A.A.A. (2021). An Assessment of ASTM E1922 for Measuring the Translaminar Fracture Toughness of Laminated Polymer Matrix Composite Materials, Polymers 2021, 13, 3129, DOI: 10.3390/POLYM13183129.
[20] El-Sagheer, I., Abd-Elhady, A.A., Sallam, H.E.D.M., Naga, S.A.R., Sayed, S.A.A. (2022). Flexural and fracture behaviors of functionally graded long fibrous polymeric composite beam-like specimens, Compos Struct, 300, p. 116140. DOI: 10.1016/J.COMPSTRUCT.2022.116140.
[21] Feng, N.L., Malingam, S.D., Jenal, R., Mustafa, Z., Subramonian, S. (2020). A review of the tensile and fatigue responses of cellulosic fibre-reinforced polymer composites, Mechanics of Advanced Materials and Structures, 27(8), pp. 645–660. DOI: 10.1080/15376494.2018.1489086.
[22] Gómez, S., Ramón, B.B., Guzman, R. (2018). Estudio comparativo de las propiedades mecánicas y vibratorias de un material compuesto reforzado con fibras de fique frente a un compuesto con fibras de vidrio – E, Revista UIS Ingenierías, 17(1), pp. 43–50. DOI: 10.18273/REVUIN.V17N1-2018004.

[23] Gómez-Suarez, S.A., Córdoba-Tuta, E. (2022). Composite materials reinforced with fique fibers – a review, Revista UIS Ingenierías, 21(1), p. undefined-undefined. DOI: 10.18273/REVUIN.V21N1-2022013.
[24] González-Estrada, O.A., Díaz, G., Quiroga, J. (2018). Mechanical response and damage of woven composite materials reinforced with fique, Key Eng Mater, 774 KEM, pp. 143–148. DOI: 10.4028/WWW.SCIENTIFIC.NET/KEM.774.143.
[25] Goumghar, A., Assarar, M., Zouari, W., Azouaoui, K., El Mahi, A., Ayad, R. (2022). Study of the fatigue behaviour of hybrid flax-glass/epoxy composites, Compos Struct, 294. DOI: 10.1016/J.COMPSTRUCT.2022.115790.
[26] Haggui, M., El Mahi, A., Jendli, Z., Akrout, A., Haddar, M. (2019). Static and fatigue characterization of flax fiber reinforced thermoplastic composites by acoustic emission, Applied Acoustics, 147, pp. 100–110. DOI: 10.1016/J.APACOUST.2018.03.011.
[27] Huelsbusch, D., Jamrozy, M., Frieling, G., Mueller, Y., Barandun, G.A., Niedermeier, M., Walther, F. (2017). Comparative characterization of quasi-static and cyclic deformation behavior of glass fiber-reinforced polyurethane (GFR-PU) and epoxy (GFR-EP), Materialpruefung/Materials Testing, 59(2), pp. 109–117. DOI: 10.3139/120.110972.
[28] Jeannin, T., Gabrion, X., Ramasso, E., Placet, V. (2019). About the fatigue endurance of unidirectional flax-epoxy composite laminates, Compos B Eng, 165, pp. 690–701. DOI: 10.1016/J.COMPOSITESB.2019.02.009.
[29] Kurien, R.A., Santhosh, A., Paul, D., Kurup, G.B., Reji, G.S. (2021). A Review on Recent Developments in Kenaf, Sisal, Pineapple, Bamboo and Banana Fiber-Reinforced Composites, Lecture Notes in Mechanical Engineering, pp. 301–310. DOI: 10.1007/978-981-16-0909-1_30.
[30] Liang, S., Gning, P.B., Guillaumat, L. (2014). Properties evolution of flax/epoxy composites under fatigue loading, Int J Fatigue, 63, pp. 36–45. DOI: 10.1016/J.IJFATIGUE.2014.01.003.
[31] Liang, S., Gning, P.B., Guillaumat, L. (2012). A comparative study of fatigue behaviour of flax/epoxy and glass/epoxy composites, Compos Sci Technol, 72(5), pp. 535–543. DOI: 10.1016/J.COMPSCITECH.2012.01.011.
[32] Mahboob, Z., Bougherara, H. (2018). Fatigue of flax-epoxy and other plant fibre composites: Critical review and analysis, Compos Part A Appl Sci Manuf, 109, pp. 440–462. DOI: 10.1016/J.COMPOSITESA.2018.03.034.
[33] Mahboob, Z., Bougherara, H. (2020). Strain amplitude controlled fatigue of Flax-epoxy laminates, Compos B Eng, 186. DOI: 10.1016/J.COMPOSITESB.2020.107769.
[34] Mahboob, Z., Fawaz, Z., Bougherara, H. (2022). Fatigue behaviour and damage mechanisms under strain controlled cycling: Comparison of Flax–epoxy and Glass–epoxy composites, Compos Part A Appl Sci Manuf, 159. DOI: 10.1016/J.COMPOSITESA.2022.107008.
[35] Muñoz, M., Salazar, M., hernandez, J. (2014). Fibras de fique una alternativa para el reforzamiento de plásticos. influencia de la modificación superficial, 12(2), pp. 60–70.
[36] Pertuz, A.D., Díaz-Cardona, S., González-Estrada, O.A. (2020). Static and fatigue behaviour of continuous fibre reinforced thermoplastic composites manufactured by fused deposition modelling technique, Int J Fatigue, 130. DOI: 10.1016/J.IJFATIGUE.2019.105275.
[37] Rajak, D.K., Pagar, D.D., Menezes, P.L., Linul, E. (2019). Fiber-reinforced polymer composites: Manufacturing, properties, and applications, Polymers (Basel), 11(10). DOI: 10.3390/POLYM11101667/.
[38] Shaghaleh, H., Xu, X., Wang, S. (2018). Current progress in production of biopolymeric materials based on cellulose, cellulose nanofibers, and cellulose derivatives, RSC Adv, 8(2), pp. 825–842. DOI: 10.1039/C7RA11157F.
[39] Shah, D.U. (2016). Damage in biocomposites: Stiffness evolution of aligned plant fibre composites during monotonic and cyclic fatigue loading, Compos Part A Appl Sci Manuf, 83, pp. 160–168. DOI: 10.1016/J.COMPOSITESA.2015.09.008.
[40] Shah, D.U., Schubel, P.J., Clifford, M.J., Licence, P. (2013). Fatigue life evaluation of aligned plant fibre composites through S-N curves and constant-life diagrams, Compos Sci Technol, 74, pp. 139–149. DOI: 10.1016/J.COMPSCITECH.2012.10.015.
[41] Sharma, A., Sharma, P., Sharma, A., Tyagi, R., Dixit, A. (2017). Hazardous Effects of Petrochemical Industries: A Review, Recent Advances in Petrochemical Science, 3(2), DOI: 10.19080/RAPSCI.2017.03.555607.
[42] Taimour, M., Abd-Elhady, A.A., Sallam, H.E.D.M., Sayed, S.A.A. (2023). Implementing functionally graded fibers technique to enhance pinned-joint performance in cross-ply laminate polymeric composites, Compos Struct, 313, p. 116931. DOI: 10.1016/J.COMPSTRUCT.2023.116931.
[43] Talreja, R., Varna, J. (2015). Modeling damage, fatigue and failure of composite materials, Modeling Damage, Fatigue and Failure of Composite Materials, pp. 1–454. DOI: 10.1016/C2013-0-16521-X.
[44] Varghese, A.M., Mittal, V. (2017). Surface modification of natural fibers, Biodegradable and Biocompatible Polymer Composites: Processing, Properties and Applications, pp. 115–155. DOI: 10.1016/B978-0-08-100970-3.00005-5.